Some Problems of Fatigue Crack Propagation in Marine Structures under Seaway Loading

Y. Sumi

Faculty of Engineering, Yokohama National University
79-5 Tokiwadai, Hodogaya-ku, Yokohama 240-8501, Japan
e-mail: sumi@ynu.ac.jp

ABSTRACT. *In order to prevent the initiation of a brittle crack in a marine structure, fatigue crack propagation from potentially hazardous embedded weld defects must be evaluated under the realistic seaway loading using a certain clustered loading pattern. We first simulate the fatigue crack propagation under the random sequence of clustered loading so-called Storm Model. The numerical simulation is carried out by a method considering the plastic wake on the crack surfaces, which may cause the retardation effects after high amplitude of loading. Furthermore, fatigue crack propagation under the effect of slam-induced whipping stress is examined by a series of experiments using CT specimens.*

INTRODUCTION

The rapid size-increase of container ships has lead to the application of extremely thick steel plate (the thickness range of 50-75mm) in the deck structures such as hatch side coaming, upper deck and other structural members in order to satisfy the requirement of longitudinal strength (strength as a ship beam). Recent researches have revealed that current structural design does not necessarily have the satisfactory background data for the structural integrity of the large container ships constructed by using these extremely thick plates[1)]. This may lead to some concerns about the fracture toughness of welded joint, which is thicker than 50mm, because fracture toughness along the butt-welded joint was formerly investigated for plates with moderate thickness. It is of our immediate interest to reconsider the possible scenarios of crack propagation and arrest behavior in ship structures, whose possible paths may include the one illustrated in Fig.1.

Also, the detection of weld-defects during the construction stage of a vessel and fatigue crack detection by periodical in-service inspections are essential to prevent brittle fracture, where fatigue crack propagation from embedded flaws in the weld under realistic seaway loading must be predicted for the proper determination of the acceptable size of the initial defects and the maximum inspection interval based on fracture mechanics approach [1,2)] (see Fig.2). In the present paper, investigations are

made for the fatigue crack growth subjected to random sequence of clustered loading, which simulates a certain seaway loading. Numerical computations are carried out for the crack growth in thick plates of deck structures. Further discussions are also made for the retardation effects, experimental verifications, and the effects of slam-induced whipping stress.

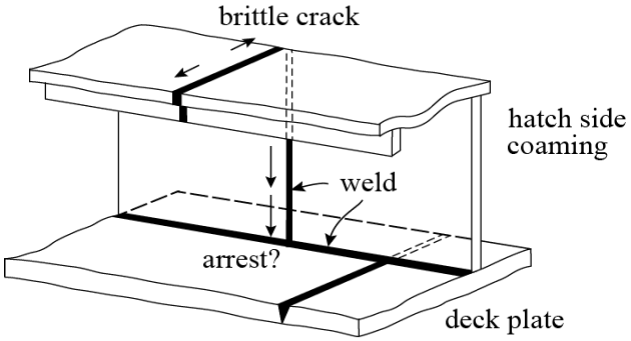

Figure 1. Possible crack path of brittle fracture in a deck structure.

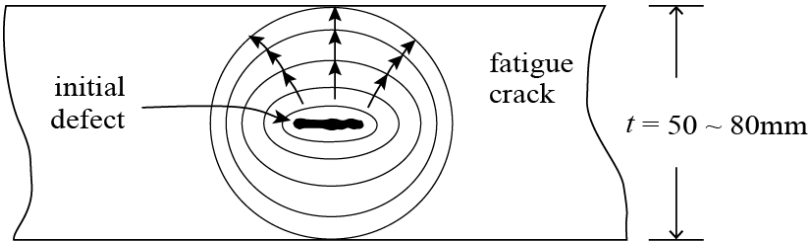

Figure 2. Fatigue crack growth from an internal defect in extremely thick welded joint.

FATIGUE CRACK PROPAGATION IN A THICK PLATE UNDER RANCOM SEQUENCE OF CLUSTERED LOADING

Modeling of an Embedded Crack and Random Sequence of Clustered Loading

In the present paper, fatigue crack propagation from an initial elliptical defect is investigated, which is assumed to locate in the middle thickness of the plate and to be subjected to repeated stresses (see Fig.3). The stress intensity factors at the ends of the major and minor axes of the ellipse can be evaluated by an empirical formula [3].

A random sequence of cluster loading is simulated by the so-called storm-model[4, 5]. We generated six clustered load patterns A, B, C, D, E, and F as illustrated in Fig.4, in which each clustered loading sequence consists of 48,000 loading cycles of gradually increasing and decreasing stress amplitudes. The probability of occurrence of Storm A to F is defined in Table 1 so that the total spectrum of the loads satisfies a given Weibull distribution in the Northern Pacific route. During the crack growth simulation, these clustered loads are applied by numerically generated random sequences of loading

based on the probability of occurrence. The applied stress condition is assumed in such a way that the maximum stress range is 262[MPa] and the mean stress is 112[MPa], with the Weibull shape parameter, 1.0. The total number of 93 clustered loads may be interpreted as the 4464×10^3 highest cycles among the 10^8 cycles of seaway loading in 25years of service.

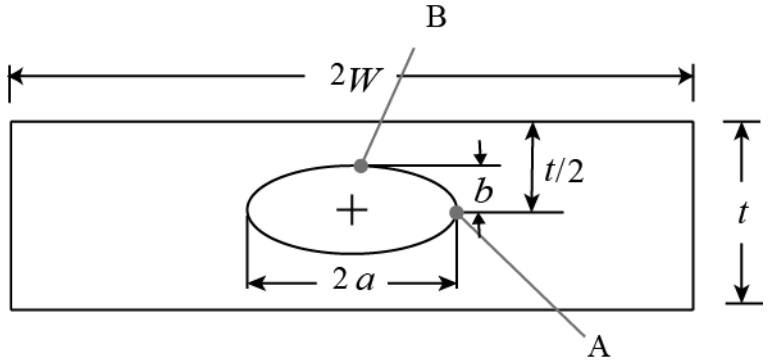

Figure 3. Embedded elliptical crack in a thick welded joint.

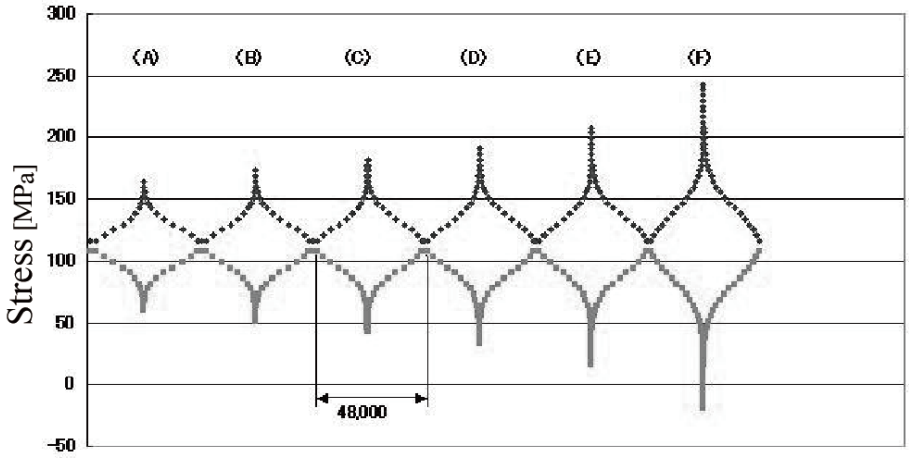

Figure 4. Clustered loading patterns A to F.

Table1: Probability of occurrence of the clustered loads A-F.

Storm	A	B	C	D	E	F
Probability	42/93	25/93	12/93	7/93	6/93	1/93

Numerical Simulation of Fatigue Crack Growth

Numerical simulations are carried out for an embedded elliptical crack propagating in a thick plate for 20 sets of random sequence of clustered loading by the two methods

based on the repeated tensile plasticity range, and the effective stress intensity range, respectively. We shall present a brief account of these methods below.

Crack growth model based on ΔK_{RP}

The main procedure of the simulation is summarized as follows;

1. calculate the stress intensity range at points A and B of the elliptical crack subjected to repeated tensile loading,
2. near-tip plastic deformation including crack opening, closure, and repeated tensile plasticity are analyzed by the strip-yielding model subjected to the k-field as the far-field boundary condition at the crack front points A and B[6],
3. the repeated tensile plasticity range of stress intensity, ΔK_{RP}, is used as the measure of the size of repeated plasticity region at each crack tip in order to calculate the crack growth rate[7, 8]
4. crack tips A and B are moved to the extended crack tip so as to form a next embedded elliptical crack, and go back to step1 to continue the simulation.

Toyosada *et al.* [7, 8] defined a load, at which the tensile yielding begins to develop ahead of a crack tip under a reloading process. The stress intensity factor corresponding to this load level is defined as k_{RP}, and the effective stress intensity range, ΔK_{RP}, is defined by

$$\Delta K_{\mathrm{RP}} = k_{\max} - k_{RP}, \tag{1}$$

where $k_{\max}$ corresponds to the stress intensity factor at the maximum load. The crack growth law based on ΔK_{RP} is expressed by

$$da / dN = C(\Delta K_{\mathrm{RP}})^m. \tag{2}$$

With regard to the mechanism of fatigue crack growth during each load cycle, there still exist several unknown phenomena. The possible difference of residual plastic wake of a fatigue crack surface is illustrated in Fig.5, in which if a fatigue crack extends during the unloading process, the crack tip may fully be stretched with its crack opening displacement denoted by $v_{\min}(x)$ (left-hand side of the figure), while if it occurs during the loading process, it may be minimized as denoted by $\tilde{v}_{\min}(x; c+\Delta c)$ (right-hand side of the figure). Possible plastic deformation during the crack growth may be assumed somewhere between these two extremes and expressed by;

$$v_{\min}(x; c+\Delta c) = (1-\kappa) v_{\min}(x) + \kappa \tilde{v}_{\min}(x; c+\Delta c), \quad 0 < \kappa < 1, \tag{3}$$

where the parameter, κ, is approximated by

$$\kappa = \begin{cases} \alpha(\gamma_e / \gamma_{pi})^n & \text{for } \alpha(\gamma_e / \gamma_{pi})^n < 1 \\ 1 & \text{for } \alpha(\gamma_e / \gamma_{pi})^n > 1, \end{cases} \tag{4}$$

The quantity, γ_e is the previously formed maximum plastic zone size, while γ_{pi} is the plastic zone size generated by the current maximum load, and α and n are the material

constants to be determined. As a result, the thickness of the residual plastic wake increases with decreasing the parameter, κ, which may play an essential role to the retardation of fatigue crack propagation.

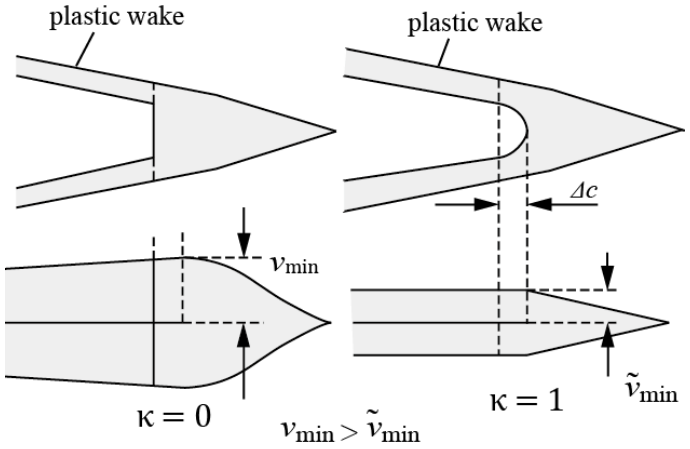

Figure 5. Mechanisms of the formation of plastic wake during fatigue crack growth

In the numerical simulations in this section, the following material constants are used; C=4.506×10^{-11}[SI-unit], m=2.692, plastic constraint factor λ=1.04, plastic wake parameters, α=0.1, n=0.1, Young's modulus E=206[GPa], Poisson's ratio ν=0.3, σ_Y=417[MPa].

Simple crack growth model

As a conventional model, we shall simply replace the above-mentioned steps 2 and 3 by the following crack growth law[9)]

$$da/dN = C\{(U \cdot \Delta K)^m - (\Delta K_{\text{eff}})_{\text{th}}^m\}, \tag{5}$$

where ΔK is the stress intensity range, C=1.411 × 10^{-11}[SI-unit], m=2.958, $(\Delta K_{\text{eff}})_{\text{th}}$ =2.58 [MPam$^{1/2}$] are the material constants. U is the effective crack opening ratio given by

$$U = \begin{cases} 1/(1.5 - R) & (-\infty \le R \le 0.5) \\ 1 & (0.5 \le R \le 1), \end{cases} \tag{6}$$

where R is the stress ratio. It should be noted that the retardation and acceleration effects of fatigue crack propagation induced by load sequences cannot be considered by this simple crack growth model.

Shape Change of the Growing Cracks

The typical shape change of the embedded crack is illustrated in Fig.6 (a) for a case of its initial shape 2a=25mm and 2b=5mm, which shows the gradual change from elliptical

to circular shape. The change of the aspect ratio of the elliptical cracks under 20 different load sequences is obtained by the crack growth model based on ΔK_{RP}, and the results are shown in Fig. 6(b). We can see from this figure that the effect of the load sequence is not so significant to the shape change of embedded cracks.

Retardation Effect of Seaway Loading

Crack propagation lives are shown in Fig.7, in which the conventional simple method estimates considerably shorter (conservative) lives than those predicted by the crack growth model based on ΔK_{RP}-criterion, because the former does not properly take into account of the increase of the thickness of plastic wake after a high level of applied stress, which apparently leads to the retardation of fatigue crack growth. The average fatigue lives obtained by ΔK_{RP}-criterion is approximately 2-3 times longer than those calculated by the simple method, and the coefficient of variance of the curves by ΔK_{RP}-criterion is less than 10% (see Table 2). Since the retardation effect may increase the scatter of fatigue crack propagation lives, we need further investigation by numerical simulation combined with experiments.

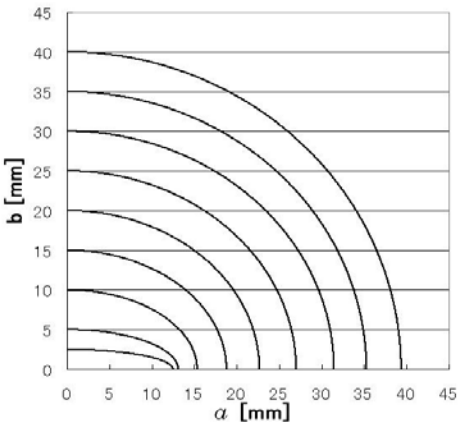

(a) crack shape

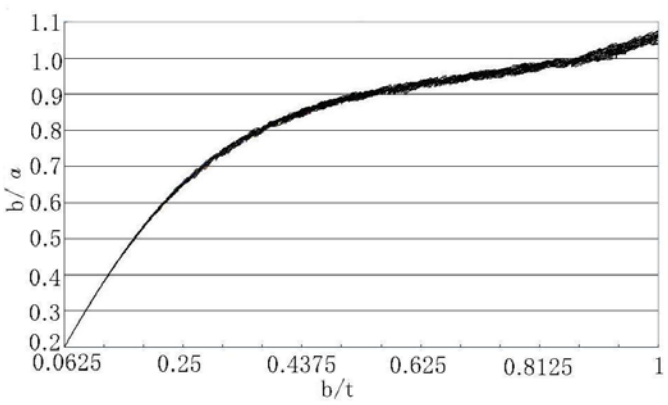

(b) aspect ratio

Figure 6. Geometric change of an embedded crack (initial crack 2*a*=25mm, 2*b*=5mm).

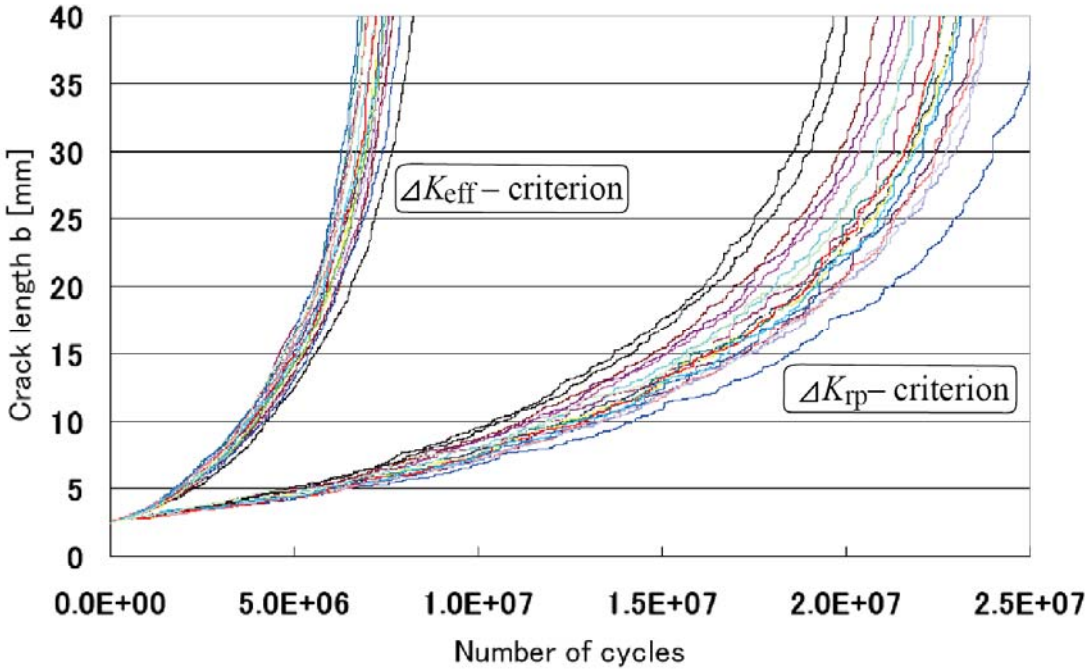

Figure 7. Varieties of simulated crack propagation life of an embedded elliptical crack. (initial crack 2*a*=25mm, 2*b* =5mm)

Table 2 Mean, standard deviation and COV of crack propagation lives (initial crack 2*a*=25mm, 2*b* =5mm)

Initial crack 2b=5mm		Crack length						
		5mm	10mm	15mm	20mm	30mm	35mm	40mm
ΔK_{eff} 20 samples	mean	1.98E+06	3.85E+06	5.03E+06	5.88E+06	6.86E+06	7.13E+06	7.33E+06
	std. dev.	1.29E+05	2.14E+05	2.49E+05	2.55E+05	3.46E+05	3.59E+05	3.78E+05
	COV	6.50E-02	5.55E-02	4.96E-02	4.35E-02	5.05E-02	5.03E-02	5.15E-02
ΔK_{rp} 20 samples	mean	5.68E+06	1.23E+07	1.62E+07	1.87E+07	2.14E+07	2.21E+07	2.25E+07
	std. dev.	5.29E+05	1.17E+06	1.39E+06	1.51E+06	1.62E+06	1.63E+06	1.65E+06
	COV	9.31E-02	9.46E-02	8.57E-02	8.09E-02	7.58E-02	7.37E-02	7.32E-02

FURTHER DISCUSSIONS

Some Considerations about Retardation Effect

In order to investigate the effect of sequence of the clustered loads and the so-called equivalent constant amplitude of loading, fatigue crack propagation is simulated for the five cases explained below and the results are illustrated in Fig.8.

Case 1 Repeated equal clustered loading
Having generated 93 sets of clustered loads based on the probability of occurrence given in Table 1, the load sequence is re-ordered to the one set of monotonically increasing and decreasing load sequence, whose load cycles are then divided by 93 to form the 93 equal clustered loads. The crack propagation life so obtained is slightly shorter than the average of the random sequence of clustered loading given in Fig.7.

Case 2 Clustered loads applied in ascending order
The 93 sets of clustered load are generated based on the probability of occurrence given in Table 1, and the load sequence is re-ordered in such a way that the clustered load level is increased from A to F in the ascending order, and this load set is repeatedly applied. The result shows a slightly longer crack propagation life compared with that of Case 1.

Case 3 Monotonically increasing load sequence
Having generated 93 sets of clustered load which is the same as Case 1, the load sequence is re-ordered to monotonically increasing order. The crack propagation life is considerably shorter than those of the previous cases as illustrated in Fig.8, because no retardation effect can be expected in this loading sequence.

Case 4 Intentionally retarded loading sequence
This is the case, where the 93 load sets are re-ordered to maximize the retardation effect by intentionally ordering the lower levels of the clustered load patterns, A and B after the higher levels of the clustered load patterns such as F and E. The result shown in Fig. 8 is obtained by repeatedly applying this load pattern.

Case 5 Equivalent constant stress range
In case of random loading, the equivalent stress range defined by

$$\Delta\sigma_{eq} = \sqrt[m]{\sum(\Delta\sigma_i^m \cdot n_i)/\sum n_i} \tag{7}$$

is commonly used to estimate the fatigue life, where $\Delta\sigma_i$ is the stress range of the *i*-th level, n_i is the corresponding load cycles, and *m* is the power of the crack propagation law, respectively. In the present case, the maximum stress, σ_{max}=137.6 [MPa], and minimum stress, σ_{min}=86.4 [MPa], and the crack propagation life so obtained is illustrated also in Fig.8, exhibiting the shortest fatigue life, because we cannot expect the retardation effect under constant amplitude loading.

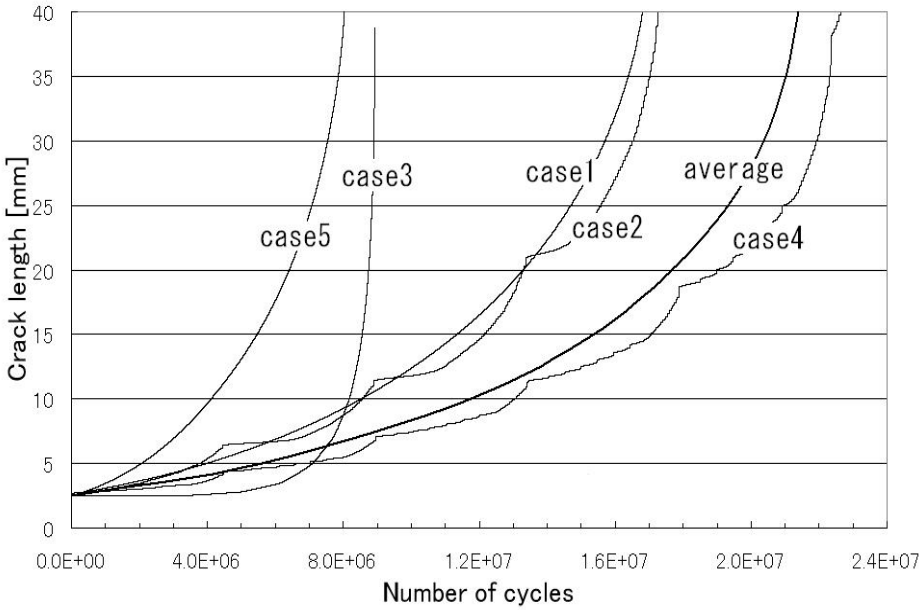

Figure 8. Comparisons of fatigue crack propagation lives under different sequence of the clustered loads (cases 1-4), equivalent constant load (case 5), and the average of the random sequence of clustered loading.

Experiments and Simulation of Fatigue Crack Propagation under Random Sequence of Clustered Loading

In order to examine the validity of the present simulation, fatigue crack propagation tests were carried out by using CT specimens (see Ref. [10] in details). In order to determine the material parameters, α and n, in Eq.4, which play an essential role to predict the realistic retardation behavior of fatigue crack growth, the material parameter, α, is first estimated by a constant amplitude test. Then, the random sequence of clustered load is applied to the same specimen to ensure the accurate determination of the material parameters, n, in Eq.4. From these experiments, we obtain α=0.015-0.020, and n=-1. Other material constants commonly used for numerical simulation are C=3.514×10^{-11}(SI units), m=2.692, and mechanical properties, E=206 [GPa], ν=0.3, the plastic constraint factor, λ=1.04, respectively.

Numerical simulations and the corresponding experiments have been carried out by using two specimens, to which the same constant amplitude load followed by the same random sequence of clustered load is applied. Even under the completely same loading sequence, the crack propagation behavior in experiments obviously exhibits a slight difference, while the difference in numerical simulation stems from the slight change of the material parameter, α (see Fig.9). These results show the very good agreement so that the proposed method can predict the fatigue crack growth behavior under the random sequence of clustered loading. It should again be noted that the estimated crack propagation lives based on the equivalent load are rather conservative.

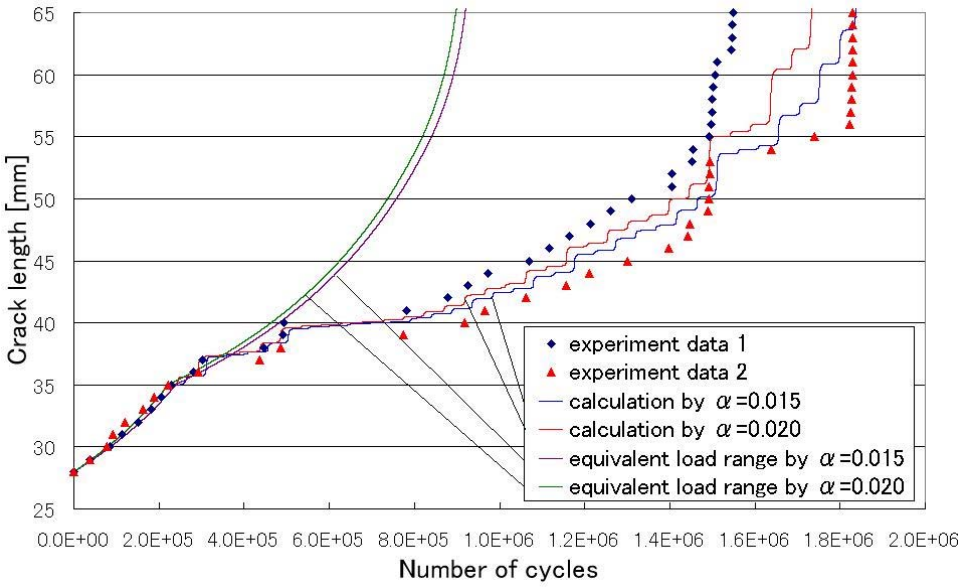

Figure9. Comparisons of experimental and simulated crack propagation lives[10].

Effect of Slam-induced Whipping Stress

In certain heavy sea conditions, marine structures are subjected to wave bending stress superimposed by slam-induced vibratory stresses. In order to study the effect of such vibratory stresses, fatigue crack propagation tests are carried out by using CT-specimens under the conditions listed in Table 3. Some loading time-histories are also illustrated in Fig.10. The results of the crack propagation lives are compared in Fig.11, in which the numerical simulations for M-0.5, M-1.0, and M-1.5 are also included for reference. The material constants are the same as those in the previous subsection except for C=1.770×10^{-11}[SI-unit] and m=2.938. It should be noted that the number of cycles in the figure is based on the low frequency load cycles.

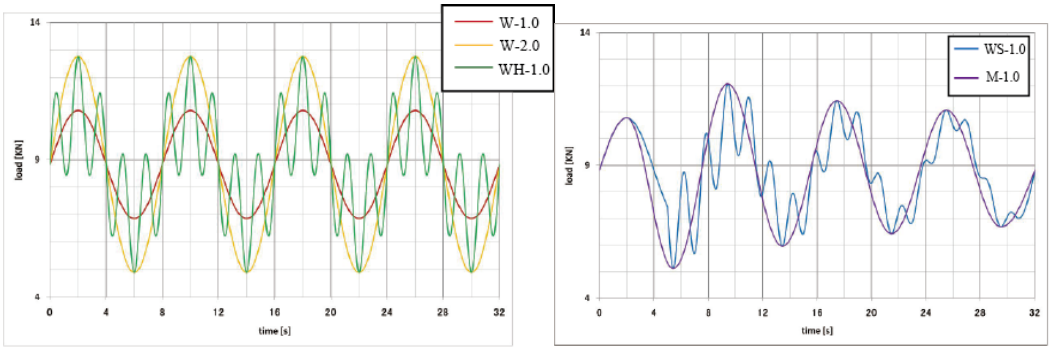

(a) (b)

Figure 10. Load histories; (a) constant amplitude tests, W-1.0 and W-2.0, and the superimposed high frequency load, WH-1.0; (b) slam-induced stress, WS-1.0, and the corresponding low frequency load, M-1.0.

Table 3. Test conditions of specimens

Specimen	Test conditions
W-1.0	Basic constant amplitude test (see Fig. 11(a))
W-2.0	Load level is twice as high as W-1.0 (see Fig. 11(a))
WH-1.0	Basic constant amplitude +high frequency constant amplitude with the same magnitude (see Fig. 11(a))
WS-1.0	Basic constant amplitude +slam-induced dynamic stress of the same amplitude (see Fig. 11(b))
M-1.0	Low frequency stress with the same maximum and minimum stresses as those of WS-1.0 (see Fig. 11(b))
WS-0.5	Basic constant amplitude +slam-induced dynamic stress of the half amplitude
M-0.5	Low frequency stress with the same maximum and minimum stresses as those of WS-0.5
WS-1.5	Basic constant amplitude +slam-induced dynamic stress of the 150% amplitude
M-1.5	Low frequency stress with the same maximum and minimum stresses as those of WS-1.5

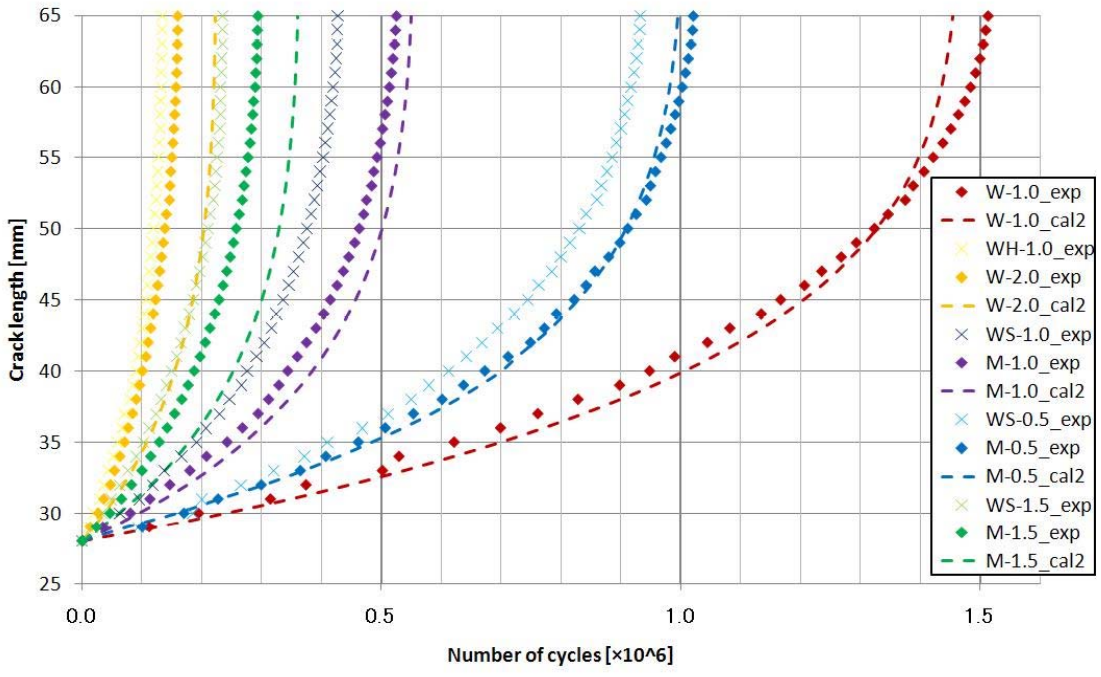

Figure 11. Comparisons of crack propagation lives for slam-induced stresses

It can be seen that the fatigue crack propagation life under slam-induced stress may be estimated from results of the M-series specimens, whose maximum and minimum stress is the same as those of slam-induced stress but the load cycles do not include the high frequencies.

CONCLUSIONS

The retardation effect of the random sequence of clustered loading has been revealed, where the predicted fatigue lives are 2-3 times longer than those predicted by the conventional method. It has also been confirmed that the present results are in good agreement with experiments and significantly influenced by the load sequence. Considerations are also made for the effect of slam-induced whipping stress.

ACKNOWLEDGEMENT

This work has been in parts supported by Grant-in-Aid for Scientific Research (No.A-22246109) from the Ministry of Education, Science, Sports and culture, and by Japan Ship Technology Research Association (JSTRA) to Yokohama National University. The author is grateful for the support.

REFERENCES

1. Sumi, Y., Yajima, H., Toyosada, M., Yoshikawa, T., Aihara, S., Matsumoto, T., Hirota, K., Hirasawa, H., Toyoda, M. and Gotoh, K. (2010). in *Proceedings of the 11th International Symposium on Practical Design of Ships and Other Floating Structures*, Vol.2: 980-989.
2. The Japan Society of Naval Architects and Ocean Engineers (2007). Report of Project Research Panel (P-10), http://www.jasnaoe.or.jp/research/dl/report_p-10.pdf, (in Japanese).
3. WES 2805 (2006). Method of Assessment for Flaws in Fusion Welded Joints with Respect to Brittle Fracture and Fatigue Crack Growth, The Japan Welding Engineering Society.
4. Tomita, Y, Toyosada, M., Sumi,Y., and Kumano, A. (1994). in *Handbook of Fatigue Crack Propagation in Metallic Structures* (Andrea Carpinteri, ed.), Elsevier, Amsterdam, 1609-1642.
5. Tomita, Y., Hashimoto, K., Osawa, N., Terai, K., Wang, Y. (2002). ASTM STP, n 1439, *Fatigue Testing and Analysis under Variable Loading Conditions*, 420-434.
6. Okawa, T. and Sumi, Y. (2008). J. Marine Science and Technology, **13**(4):416-427.
7. Toyosada, M., Gotoh, K., Niwa, T. (2004). International Journal of Fatigue **26**:983-992.
8. Toyosada, M., Gotoh, K., Niwa, T. (2004). International Journal of Fatigue **26**:993-1002.
9. Kato A, Kurihara M, Kawahara M. (1983). Journal of the Society of Naval Architects of Japan **153**:336-343 (in Japanese).
10. Sumi, Y. and Inoue, T. (2011). Marine Structures **24**(2): 117-131.